EMBEDDED ABSORBERS FOR HELICOPTER ROTOR LAG DAMPING

Lynn Byers and **Farhan Gandhi**

Rotorcraft Center of Excellence
Department of Aerospace Engineering
The Pennsylvania State University, University Park, PA 16802, USA
e-mail: fgandhi@psu.edu

Key words: rotor lag damping, chordwise and radial vibration absorber, Coriolis coupling

Abstract: Radial and chordwise damped vibration absorbers embedded in the rotor blade are compared for rotor lag damping augmentation. Results show that the radial absorber is more effective in transferring damping to the rotor blade lag mode. The chordwise absorber needs to be at a more outboard location and have a larger mass to introduce levels of lag damping comparable to that introduced by the radial absorber. The 1/rev amplitude of a chordwise absorber at the blade tip, per degree of blade lead-lag motion in forward flight, is of the order of 35% of the blade chord, and such a stroke might be difficult to accommodate. The 1/rev amplitude of a radial absorber at 70% span (having significantly lower mass than the chordwise absorber and producing comparable lag damping) is of the order of 4% span. The static displacement of the radial absorber under centrifugal (CF) loading needs to be limited using a frequency-dependent (high static stiffness, low dynamic stiffness) or nonlinear spring. The chordwise absorber can also undergo a large static displacement under the chordwise component of the CF load if there is an offset from the feather axis, and this would again have to be limited using a strategy such as a frequency-dependent spring. Significant advantages of the radial absorber are – higher lag damping, lower absorber mass, space for absorber mass travel, no chordwise travel of blade center of gravity reducing susceptibility to aeroelastic instability and dynamic pitch-link loads.

1 BACKGROUND

Helicopters with soft-inplane rotors are known to be susceptible to aeromechanical instabilities such as ground- and air-resonance, which arise due to the coupling of the poorly damped rotor cyclic lag modes with the fuselage modes. The conventional approach to alleviating these instabilities has been to ensure an adequate amount of damping in the lag mode through the provision of auxiliary lag dampers at the rotor blade root. However, associated with the use of auxiliary root-end lag dampers are issues such as increased hub complexity, aerodynamic drag, and high maintenance requirements. In recent years, hydraulic dampers have been giving way to elastomeric lag dampers. The modern elastomeric dampers are themselves expensive, susceptible to fatigue, and display complex behavior including – nonlinear amplitude dependence, frequency dependence, sensitivity to temperature with loss of damping at extremes in temperature, and blade limit cycle oscillations. Additionally, elastomeric dampers as well as the even more recent Fluidlastic® dampers can sometimes have difficulty in introducing the required levels of damping in the lag mode (as was the case with the RAH-66 Comanche).

2 EMBEDDED VIBRATION ABSORBERS FOR ROTOR LAG DAMPING

An alternative to root-end auxiliary lag dampers suggested by researchers at Penn State (Refs. 1–6) was to introduce lag mode damping through an *embedded chordwise damped vibration absorber* in the outboard region of the blade (see Figs. 1 and 2). For the correct choice of

system design parameters, it was shown that a significant amount of lag damping could be introduced, and aeromechanical stability could be improved. However, the chordwise absorber has stringent restrictions on stroke-length due to space limitations, and there are concerns that the motion of the absorber mass in the chordwise direction, which results in the movement of the blade center of gravity, can have a detrimental influence on blade aeroelastic stability (pitch-flap flutter) and potentially increase the dynamic pitch link loads. Additionally, the magnitude of the absorber mass required for satisfactory damping augmentation is quite large (of the order of 10% of the blade mass).

More recently, a *radial vibration absorber* has been proposed for its ability to augment rotor blade lag mode damping (Refs. 7–9). As depicted in the schematic in Fig. 3, the absorber mass (restrained by a damped spring) oscillates along the spanwise direction (potentially along a frictionless track within the spar). In the process, it exerts a tangential Coriolis force on the rotating blade, in the lead-lag direction. The lead-lag motion of the rotating blade (and the absorber mass), in turn, exerts a radial Coriolis force on the absorber mass (see Fig. 4). Thus, there exists a Coriolis coupling between the lead-lag motion of the blade and the radial motion of the absorber mass. For the damped absorber under consideration, a significant amount of damping can be transferred into the rotor lag mode through this strong Coriolis coupling.

Relative to the chordwise vibration absorber there are no stringent stroke restrictions for the radial vibration absorber, and Refs. 7 and 9 showed that a modest absorber mass (of the order of 1-5% of the blade mass) could introduce a substantial amount of damping in the rotor lag mode and could easily alleviate aeromechanical instabilities of a hingeless rotor helicopter. Since there is no chordwise movement of the center of gravity, susceptibility to pitch-flap flutter instabilities is also reduced.

Previous studies on the chordwise absorber (Refs. 1–6) and radial absorber (Refs. 7–9) have been carried out on different rotors, and using different absorber parameters. Using a common rotor and equivalent absorber parameters, the present study seeks to compare the performance of the chordwise and radial absorbers. In particular, the levels of lag damping achieved using both types of absorbers, and the corresponding periodic response amplitudes of the absorber masses for a periodic lead-lag motion of the blade (as would be expected in forward flight conditions), are compared.

3 ANALYSIS FOR RADIAL AND CHORDWISE VIBRATION ABSORBERS

The lag damping results presented in Ref. 3 for the chordwise absorber cannot be directly compared with the results from Ref. 7 for the radial absorber since the two absorber concepts are analyzed using different absorber parameters and on different rotors. In this paper, both chordwise and radial damped vibration absorber concepts are analyzed using similar nondimensional formulations of the differential equations of motion, and for similar ranges of absorber parameters. The results compare the amount of lag damping achieved by the radial absorber versus chordwise absorber on the *same rotor*. The study also compares the periodic absorber response amplitudes for periodic lead-lag motion of the blade.

The governing linearized, nondimensional differential equations of motion for the radial absorber are as follows:

$$\begin{bmatrix} 1+3\alpha_m(\bar{a}-\bar{e})^2 & 0 \\ 0 & 1 \end{bmatrix}\begin{Bmatrix} \ddot{\zeta} \\ \ddot{\bar{x}}_r \end{Bmatrix} + \begin{bmatrix} 0 & -6\alpha_m(\bar{a}-\bar{e}) \\ 2(\bar{a}-\bar{e}) & 2\zeta_a\alpha_f\nu_\zeta \end{bmatrix}\begin{Bmatrix} \dot{\zeta} \\ \dot{\bar{x}}_r \end{Bmatrix} + \begin{bmatrix} \nu_\zeta^2 & 0 \\ 0 & \alpha_f^2\nu_\zeta^2 \end{bmatrix}\begin{Bmatrix} \zeta \\ \bar{x}_r \end{Bmatrix} = \begin{Bmatrix} \overline{M}_\zeta \\ \bar{a} \end{Bmatrix} \tag{1}$$

In the above equations ζ and $\bar{x}_r$ are the rotor lag and the absorber radial degrees of freedom (as shown in Figs. 3 and 4), α_m is the mass ratio (ratio of absorber mass to blade mass), α_f is the frequency ratio (ratio of the absorber rotating natural frequency to the blade rotating lag frequency), $\bar{a}$ is the absorber offset from hub (non-dimensionalized by the rotor radius, *R*), and ζ_a is the absorber damping ratio. The rotor blade parameters in the above equations are ν_ζ (the non-dimensional rotating lag frequency) and $\bar{e}$ (the rotor blade hinge offset, nondimensionalized by the rotor radius). $\overline{M}_\zeta$ represents the aerodynamic lag moment.

The linearized, nondimensional equations of motion for the chordwise absorber are similarly derived using Ref. 3, resulting in the following equations:

$$\begin{bmatrix} 1+3\alpha_m(\bar{a}-\bar{e})^2 & -3\alpha_m(\bar{a}-\bar{e}) \\ -(\bar{a}-\bar{e}) & 1 \end{bmatrix}\begin{Bmatrix} \ddot{\zeta} \\ \ddot{\bar{x}}_c \end{Bmatrix} + \begin{bmatrix} 0 & -6\alpha_m\bar{a}_c \\ 2\bar{a}_c & 2\zeta_a\alpha_f\nu_\zeta \end{bmatrix}\begin{Bmatrix} \dot{\zeta} \\ \dot{\bar{x}}_c \end{Bmatrix} + \begin{bmatrix} \nu_\zeta^2 & -3\alpha_m\bar{e} \\ -\bar{e} & \alpha_f^2\nu_\zeta^2 \end{bmatrix}\begin{Bmatrix} \zeta \\ \bar{x}_c \end{Bmatrix} = \begin{Bmatrix} \overline{M}_\zeta \\ \bar{a}_c \end{Bmatrix} \tag{2}$$

In the above equation $\bar{x}_c$ is the chordwise motion of the absorber mass (Fig. 2) and $\bar{a}_c$ is the initial (undeformed) position of the absorber relative to the feathering axis of the blade (also seen in Fig. 2), both nondimensionalized by the rotor radius. The remaining absorber and rotor parameters in Eq. 2 are identical to those in Eq. 1, described above.

For both absorber concepts, the absorber rotating natural frequency is determined by the following equation:

$$\omega_a = \sqrt{\frac{k_a}{m_a} - \Omega^2} \tag{3}$$

where k_a and m_a represent the absorber stiffness and mass. Therefore, the frequency ratio, α_f, for both concepts, is as follows:

$$\alpha_f = \frac{\omega_a}{\omega_\zeta} = \sqrt{\frac{\frac{k_a}{m_a} - \Omega^2}{\omega_{\zeta 0}^2 + e\frac{S_\zeta}{I_\zeta}\Omega^2}} \tag{4}$$

As seen in Eqs. 3 and 4, both the absorber rotating natural frequency and the lag natural frequency are functions of rotor speed, Ω. Consequently, for fixed values for the absorber stiffness, k_a, and mass, m_a, the absorber frequency can only be "tuned" to the lag frequency (α_f = 1) at a single value of Ω.

For both systems of equations by setting the forcing terms on the right-hand side to zero and conducting an eigenanalysis, the modal damping of the coupled rotor lag and absorber modes can be calculated. Further, by introducing a harmonic excitation force for the lag equation of motion, frequency response functions for the absorber displacement, $\bar{x}_r$ and $\bar{x}_c$, and blade lag displacement, ζ, can be obtained. The frequency response functions can then be used to calculate the amplitude of the absorber displacement (or the stroke-length of the absorber mass) per degree amplitude of blade lag motion, when the blade is undergoing periodic lead-lag motion in forward flight conditions.

4 RESULTS AND DISCUSSION

The absorber parameters used for the simulation results presented in this section are given in Table 1.

Table 1: Absorber parameters used in simulations

Absorber Parameter	**Values Considered**
$\bar{a}$	0.3, 0.5, 0.7
ζ_a	0.3, 0.5, 0.7
α_f	0.5 – 1.5
α_m	.01, .02, .03, .04, .05

The rotor nondimensional lag frequency, ν_ζ, is taken to be 0.7/rev, which is typical of a soft-inplane hingeless rotor, and $\bar{e}$ = 0. Further, for the chordwise absorber, $\bar{a}_c$ = 0.

Figures 5a–7a show the modal damping results, versus frequency ratio, for a moderately damped absorber (ζ_a = 0.3) at inboard ($\bar{a}$ = 0.3, Fig. 5a), mid-span ($\bar{a}$ = 0.5, Fig. 6a), and outboard ($\bar{a}$ = 0.7, Fig. 7a) spanwise locations. For the radial absorber it is observed that the maximum damping transferred to the lag mode is 15% (one half the damping in the absorber mode), when α_f = 1. For an inboard location of the absorber (Fig. 5a), the actual damping in the lag mode depends on the absorber mass ratio, α_m, and while the ceiling value of 15% is reached for α_m = 5%, the damping in the lag mode is lower for smaller values of absorber mass ratio. As the absorber moves to mid-span and outboard locations (Figs. 6a and 7a), the damping levels in the lag mode reach the ceiling value of 15% even for smaller absorber mass ratios. In fact, for $\bar{a}$ = 0.7 (Fig. 7a), even with an absorber mass that is only 1% of the blade mass, a maximum of 15% damping in the rotor lag mode can be achieved. The lag mode damping with the chordwise absorber is considerably lower, in all cases. For the inboard location ($\bar{a}$ = 0.3, Fig. 5a) a maximum of 1.1% damping is observed in the lag mode, for the mid-span location ($\bar{a}$ = 0.5, Fig. 6a) a maximum of 3.3% damping is observed, and for the outboard location ($\bar{a}$ = 0.7, Fig. 7a) a maximum of 7.5% damping is observed – but only for the highest absorber mass ratio (α_m = 5%) considered. For lower values of α_m the lag damping with the chordwise absorber considerably decreases. In contrast, with the radial

absorber, damping of up to 15% is achieved with absorber mass ratios as low as 1%, and even when the absorber is not at the outermost spanwise location.

Figures 8a–13a show similar results for higher damped absorbers. Figures 8a–10a correspond to $\zeta_a = 0.5$, and Figs. 11a–13a correspond to $\zeta_a = 0.7$. For the radial absorber, the maximum damping in the lag mode increases to 25% (when $\zeta_a = 0.5$) and to 35% (when $\zeta_a = 0.7$). However, to reach these higher ceiling values, larger absorber mass ratios and more outboard absorber locations are generally required. For example, it is seen in Figs. 8a–10a that for the inboard location (Fig. 8a) the ceiling damping in the lag mode could not be achieved, but as the absorber moved outboard (Figs. 9a and 10a) and the mass ratios became larger, up to 25% damping was introduced in the lag mode. In contrast, for the moderately damped absorber (ζ_a = 0.3), the ceiling damping of 15% in the lag mode could be achieved even for an inboard absorber location (Fig. 5a) and for low absorber mass ratios (Figs. 6a and 7a). The performance of highly-damped chordwise absorbers (in terms of their ability to transfer damping to the rotor lag mode) is very poor compared to that of the radial absorbers (as seen from Figs. 8a–13a). Even when the chordwise absorber is at the outermost location ($\bar{a}$ = 0.7) and has the maximum mass (α_m = 5%), it transfers damping to the rotor lag mode more effectively when it is lightly- to moderately damped (ζ_a = 0.3). This is evident by comparing Fig. 7a to Figs. 10a and 13a.

By introducing a harmonic excitation force on the right hand side of the lag equation of motion for the coupled rotor lag – radial absorber system (Eq. 1) and the rotor lag – chordwise absorber system (Eq. 2), Frequency Response Functions (FRFs) for the absorber degrees-of-freedom, $\bar{x}_r$ and $\bar{x}_c$, and blade lag displacement, ζ, can be obtained. Of particular interest is the dynamic displacement amplitude of the absorber at a frequency of 1*/rev*, the dominant excitation frequency in forward flight. The radial absorber response is presented as a percentage of the blade radius, and the chordwise absorber response is presented as a percentage of the blade chord, both per degree of blade lead-lag motion amplitude. It is assumed that the blade has a notional chord length of 8% of the radius. The radial and chordwise absorber response results are shown in Figs. 5b – 13b.

In general it is observed that as the absorber moves outboard (compare Figs. 5b–7b, or 8b–10b, or 11b–13b), the absorber response amplitude increases. However, outboard absorbers were seen to introduce more lag damping than inboard absorbers. For a moderately damped absorber (ζ_a = 0.3) at an outboard spanwise location ($\bar{a} = 0.7$), the periodic response amplitude of the radial absorber was about 4% blade radius and that of the chordwise absorber was about 25% chord, per degree of blade lead-lag motion amplitude (as seen in Fig. 7b). If the chord length is a smaller fraction of the radius, the response amplitude of the chordwise absorber becomes an even greater percentage of the chord length. As the absorber damping increases, the periodic absorber response amplitude generally decreases (compare Figs. 8b–10b for $\zeta_a = 0.5$, and Figs. 11b–13b for $\zeta_a = 0.7$, to Figs. 5b–7b for ζ_a = 0.3). While highly-damped chordwise absorbers were not particularly effective in augmenting lag damping, highly-damped radial absorbers at outboard locations performed well. Thus a highly-damped, outboard radial absorber may be an interesting possible candidate design to introduce high lag damping while having limited periodic response.

Recently, rotor lag damping augmentation using a chordwise absorber located at the tip of the rotor blade has been considered (Refs. 4–6). Figure 14 shows a comparison of the

performance of the chordwise and radial absorbers located at the rotor tip, for the case of absorber damping ratio, $\zeta_a = 0.3$. As seen in Figure 14a, at this location, the chordwise absorber is able to achieve approximately 15% lag mode damping when the absorber mass is 4–5% of the blade mass. With the radial absorber smaller mass ratios, as low as 1% of the blade mass, result in similar damping levels in the rotor lag mode. Although a radial absorber "at" the blade tip is impractical (stroke requirements would necessitate that the "absorber device" extend beyond the blade tip and it would no longer be "embedded" in the blade), the radial absorber even at mid-span ($\bar{a}$ = 0.5) and at 70% span ($\bar{a}$ = 0.7) transferred as much damping to the lag mode with smaller absorber mass ratios of α_m = 1–2% (Figs. 6a and 7a). Figure 14b shows that for the chordwise absorber at the tip, its chordwise motion amplitude (periodic response) per degree of blade lag motion is over ±37% of the chord (which may again not be feasible in an "embedded" configuration). In contrast, the response of the radial absorber is approximately ±6% of the radius.

5 ABSORBER MASS STATIC DISPLACEMENT UNDER CENTRIFUGAL LOAD

The results shown in Figs. 5b–14b consider only the dynamic component of the absorber response. However, the total response of the absorber contains a static component and a dynamic component. A major factor in the implementation of a radial absorber concept is the large centrifugal force field in which the absorber will be required to operate. The static displacement of the radial vibration absorber due to the centrifugal force is dependent on the rotor speed, the radial offset of the absorber from the hub, the absorber mass, and the absorber spring stiffness as shown below.

$$\bar{x}_{r_{static}} = \frac{\bar{a}\Omega^2}{\frac{k_a}{m_a} - \Omega^2} = \frac{\bar{a}\Omega^2}{\omega_a^2} = \frac{\bar{a}}{\alpha_f^2 \nu_\zeta^2} \tag{5}$$

Using the spring stiffness required to achieve the desired tuning to the lag natural frequency (α_f = 1) results in the prediction of an unrealistically large static displacement. In practice, either the absorber spring would fail or the absorber mass would essentially get "pegged" against an outer constraint in the rotor blade. This problem could be overcome in one of two ways: An absorber spring with a frequency-dependent stiffness could be used (with a high static stiffness to withstand the centrifugal force, but a low dynamic stiffness to achieve the desired tuning to the lag frequency of the blade). Alternatively, a nonlinear softening spring can be used such that the large initial stiffness results in modest deflection under centrifugal loading but the softening of the spring thereafter allows for dynamic motion and energy dissipation (the tangent stiffness of the softer part is selected such that the absorber is dynamically tuned to the rotor lag frequency).

For the chordwise absorber, the static displacement can be determined using the equation given below.

$$\bar{x}_{c_{static}} = \frac{\bar{a}_c\Omega^2}{\frac{k_a}{m_a} - \Omega^2} = \frac{\bar{a}_c\Omega^2}{\omega_a^2} = \frac{\bar{a}_c}{\alpha_f^2 \nu_\zeta^2} \tag{6}$$

Equation 6 gives the static displacement of the chordwise absorber non-dimesionalized by the blade chord if the offset, $\bar{a}_c$, of the absorber relative to the feathering axis is also non-dimensionalized by the blade chord.

In Ref. 3 it was emphasized that for chordwise offsets, $\bar{a}_c$ in excess of 10% of the blade chord, the static displacement under the chordwse component of the centrifugal load could be unacceptably large. For this reason, development of a Fluidlastic® chordwise vibration absorber was pursued (Refs. 4–6) which could provide a high static stiffness and a lower dynamic stiffness.

6 SUMMARY

In this paper the potential of radial and chordwise damped vibration absorbers embedded in the rotor blade have been compared for rotor lag damping augmentation. The comparisons have been made on the same rotor and over a similar range of absorber parameters. Further, the 1/rev periodic response amplitude of the absorber mass per degree of blade lead-lag motion has been compared for both absorber concepts. The radial absorber, which transfers damping to the rotor blade lag mode via Coriolis coupling, is of interest as it does not face the stroke restrictions of the chordwise absorber, generally requires lower absorber mass and is potentially less susceptible to aeroelastic instabilities and dynamic pitch-link loads as it does not involve the chordwise motion of the blade center of gravity.

The conclusions drawn from the results presented in this paper are described below. The radial absorber is generally far more effective in transferring damping to the rotor blade lag mode. For comparable performance, the chordwise absorber must either use a significantly larger mass or be positioned further outboard on the rotor blade. For both absorber concepts, for damping of the order of 30% critical in the absorber mode, the amount of damping transferred to the lag mode generally increased as the absorber moved outboard and the absorber mass increased. However, for the radial absorber, the maximum amount of damping (one half of the absorber mode damping) could be transferred to the lag mode even when the absorber was at mid-span and 70% span, and for mass-ratios as low as 1–2%. In contrast, for the chordwise absorber, to transfer the maximum damping to the rotor lag mode, the absorber had to be located at the blade tip and its mass had to be 5% of the blade mass. If the absorber had higher damping, an even larger amount of damping could be transferred to the rotor lag mode in the radial configuration (especially with more outboard locations and slightly higher mass ratios). However, this was not possible in the chordwise configuration.

For a radial absorber located at 70% span, with 30% absorber mode damping, and 1% mass ratio, producing 15% damping in the lag mode, the 1/rev periodic response amplitude in forward flight was predicted to be of the order of 4% of the blade span per degree of blade lead-lag motion. In contrast, for a chordwise absorber located at the blade tip, with 30% absorber mode damping, and 5% mass ratio, producing a similar 15% damping in the lag mode, the 1/rev periodic response amplitude in forward flight was predicted to be of the order of 35% of the blade chord per degree of blade lead-lag motion. Such a large stroke may be difficult to accommodate for a chordwise absorber.

The static displacement of a radial absorber dynamically tuned to the rotor lag frequency would be unacceptably high under the centrifugal (CF) loads. This problem can potentially be alleviated by using a frequency-dependent absorber spring with a high static stiffness and a low dynamic stiffness, or a nonlinear spring initially stiff to withstand the CF loads and

subsequently softening to allow absorber dynamic motion and energy dissipation. For the chordwise absorber, its offset relative to the feather axis has to be kept small. Alternatively, a frequency-dependent spring can limit the static displacement under the chordwise component of CF loads.

7 REFERENCES

[1] Hebert, C., and Lesieutre, G., "Rotorcraft Blade Lag Damping using Highly Distributed Tuned Vibration Absorbers," *Proc. of the 39th AIAA/ASME/ASCE/AHS/ASC Structures, Structural Dynamics, and Materials Conference*, Long Beach, CA, April 20-23,1998.

[2] Kang, H., Smith, E., and Lesieutre, G., "Helicopter Blade Lag Damping Using Embedded Chordwise Absorbers," *Proceedings of the 57th Forum of the AHS*, Washington DC, May 9-11, 2001.

[3] Kang, H., "Blade Lag Damping Using Embedded Chordwise Absorbers", Ph.D. Thesis, The Pennsylvania State University, August 2001.

[4] Petrie, J., "Helicopter Rotor Blade Lag Damping Using Fluid Elastic Embedded Chordwise Inertial Dampers", MS Thesis, The Pennsylvania State University, August 2004.

[5] Petrie, J., Lesieutre, G., and Smith, E., "Helicopter Blade Lag Damping using Embedded Fluid Elastic Inertial Dampers," *Proc. of the 45th AIAA/ASME/ASCE/AHS/ASC Structures, Structural Dynamics and Materials Conference*, Palm Springs, CA, April 2004.

[6] Petrie, J., Lesieutre, G., and Smith, E., "Design and Model Testing of Helicopter Rotor Blade Lag Fluid Elastic Embedded Chordwise Inertial Dampers," *Presented at the American Helicopter Society 61st Annual Forum*, Grapevine, TX, June 1-3, 2005.

[7] Byers, L. and Gandhi, F. "Helicopter Rotor Lag Damping Augmentation Based on a Radial Absorber and Coriolis Coupling," *Presented at the American Helicopter Society 61st Annual Forum*, Grapevine, TX, June 1-3, 2005.

[8] Byers, L. and Gandhi, F. "Rotor Blade with Radial Absorber (Coriolis Damper) - Loads Evaluation," *Presented at the American Helicopter Society 62nd Annual Forum*, Phoenix, AZ, May 9-11, 2006.

[9] Byers, L., "Helicopter Rotor Lag Damping Augmentation Based on a Radial Absorber and Coriolis Coupling", Ph.D. Thesis, The Pennsylvania State University, August 2006.

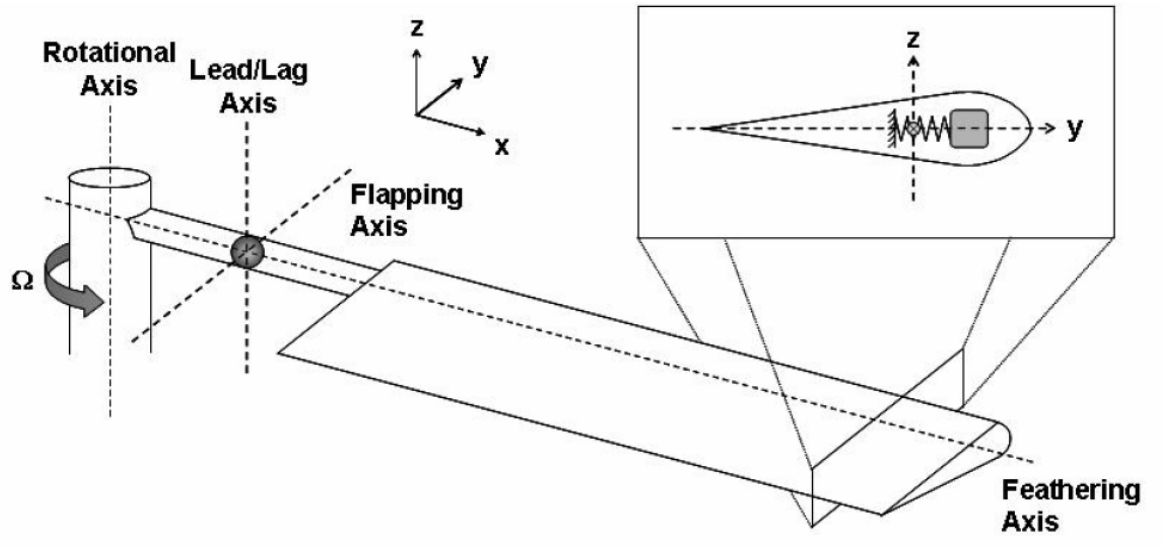

Figure 1: Embedded chordwise damped vibration absorber [4]

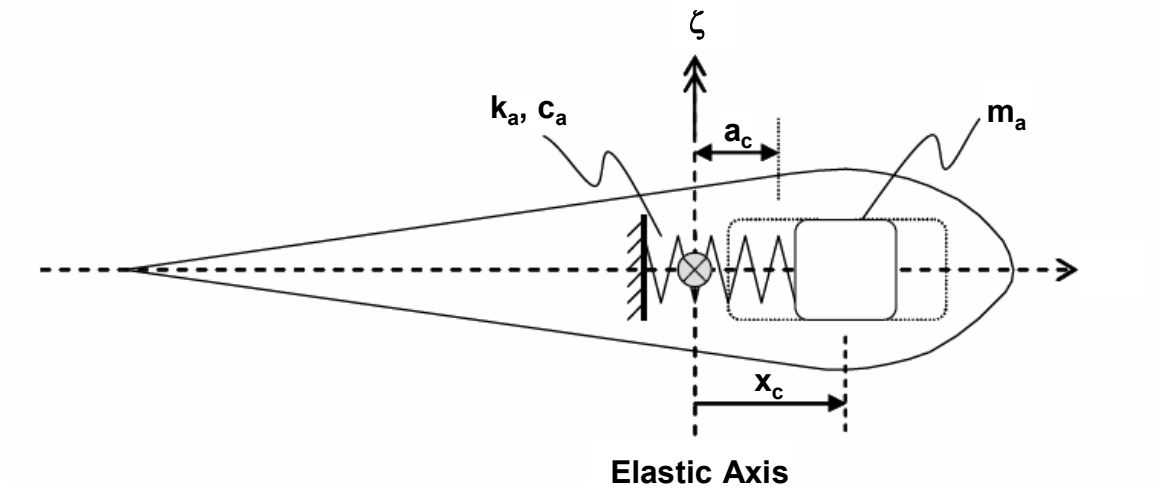

Figure 2: Embedded chordwise vibration absorber schematic (redrawn from [6])

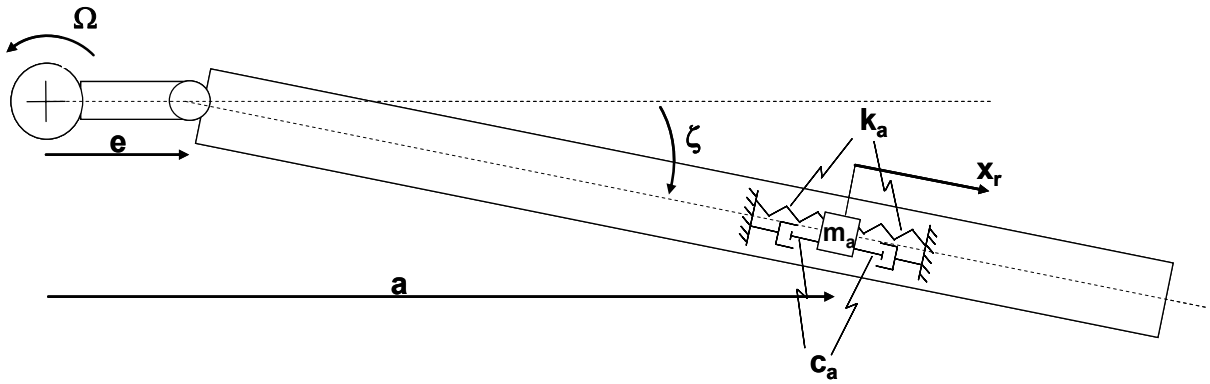

Figure 3: Embedded radial vibration absorber schematic

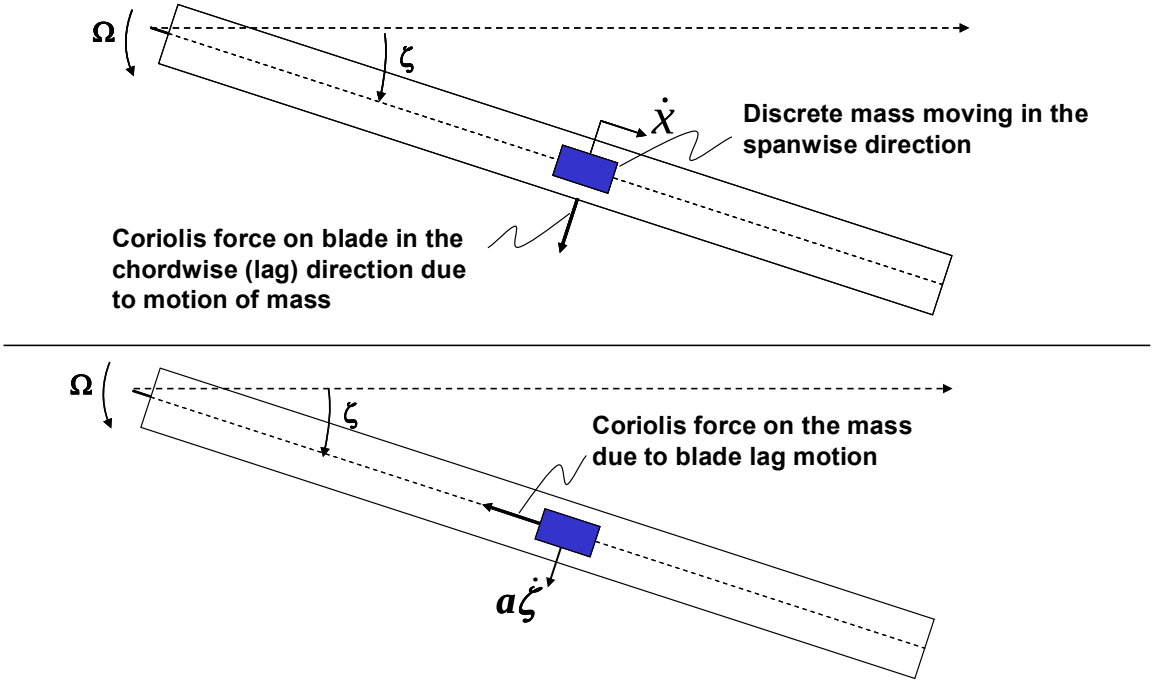

Figure 4: Coriolis force on blade and absorber mass

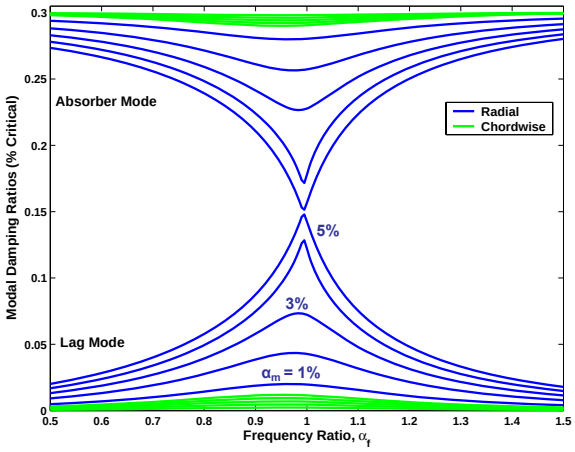

Figure 5a: Modal damping ratios vs frequency ratio, α_f ($\bar{a} = 0.3$ and $\zeta_a = 0.3$)

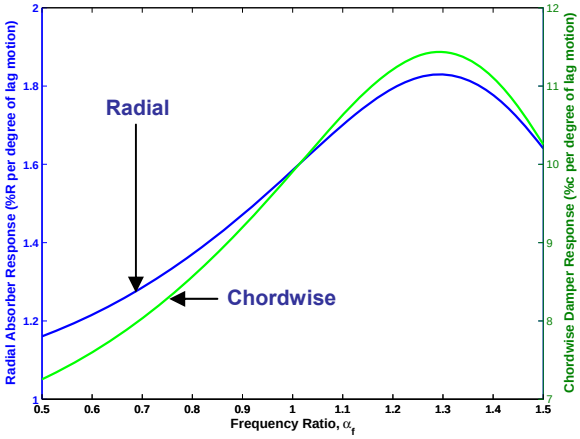

Figure 5b: 1/rev absorber amplitude per degree of lag motion ($\bar{a} = 0.3$ and $\zeta_a = 0.3$)

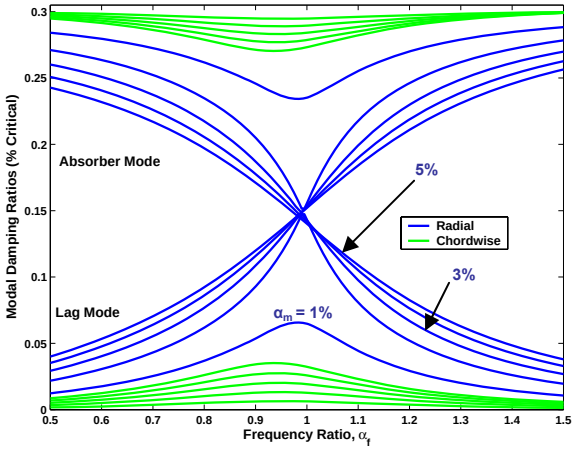

Figure 6a: Modal damping ratios vs frequency ratio, α_f ($\bar{a} = 0.5$ and $\zeta_a = 0.3$)

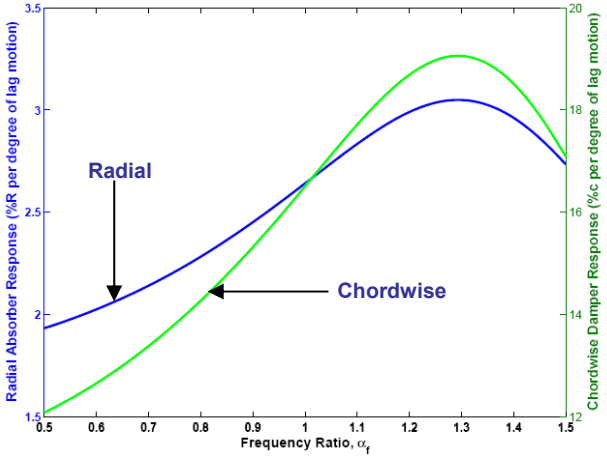

Figure 6b: 1/rev absorber amplitude per degree of lag motion ($\bar{a} = 0.5$ and $\zeta_a = 0.3$)

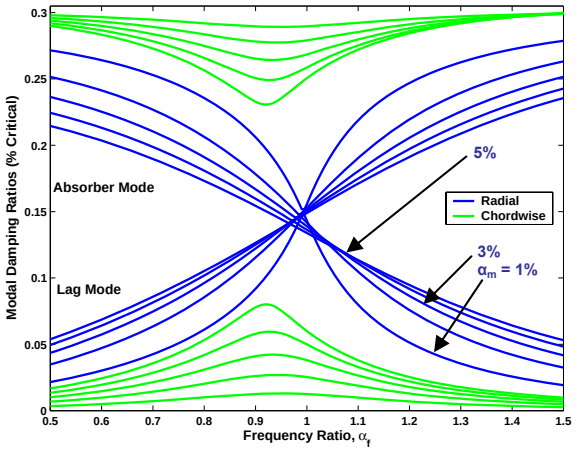

Figure 7a: Modal damping ratios vs frequency ratio, α_f ($\bar{a} = 0.7$ and $\zeta_a = 0.3$)

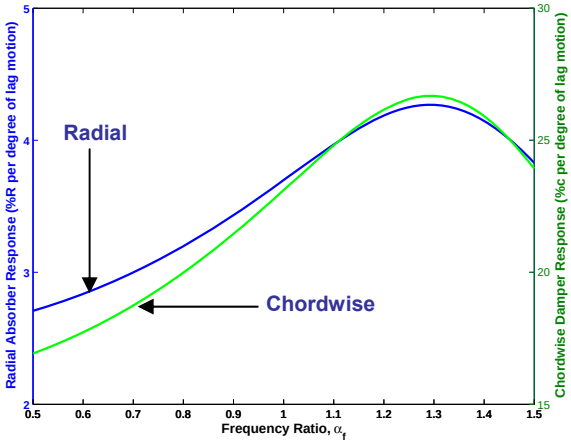

Figure 7b: 1/rev absorber amplitude per degree of lag motion ($\bar{a} = 0.7$ and $\zeta_a = 0.3$)

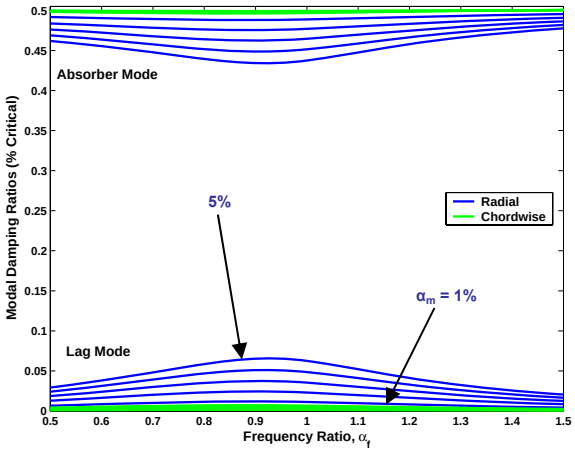

Figure 8a: Modal damping ratios vs frequency ratio, α_f ($\bar{a} = 0.3$ and $\zeta_a = 0.5$)

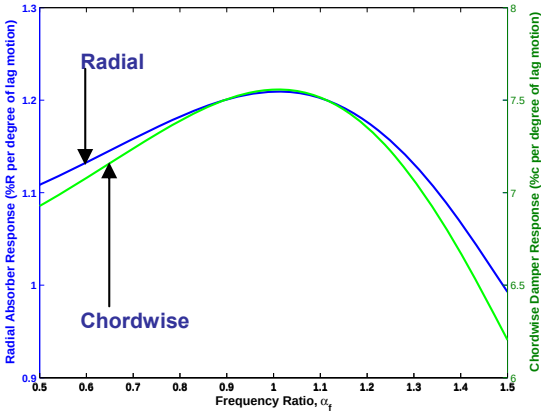

Figure 8b: 1/rev absorber amplitude per degree of lag motion ($\bar{a} = 0.3$ and $\zeta_a = 0.5$)

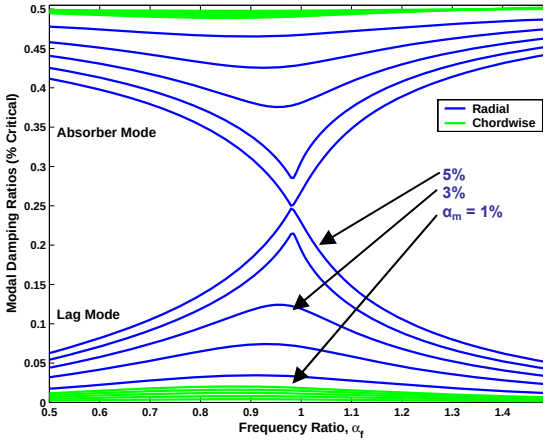

Figure 9a: Modal damping ratios vs frequency ratio, α_f ($\bar{a} = 0.5$ and $\zeta_a = 0.5$)

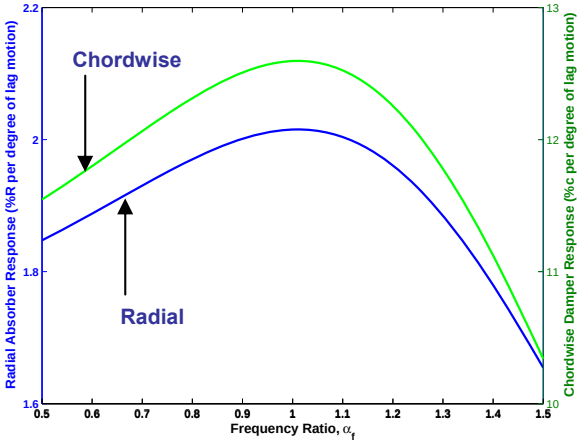

Figure 9b: 1/rev absorber amplitude per degree of lag motion ($\bar{a} = 0.5$ and $\zeta_a = 0.5$)

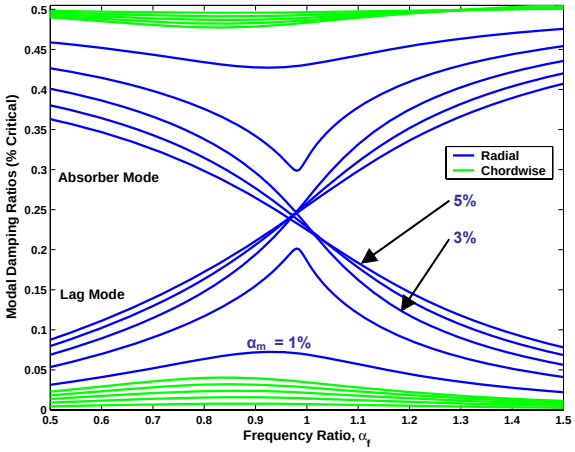

Figure 10a: Modal damping ratios vs frequency ratio, α_f ($\bar{a} = 0.7$ and $\zeta_a = 0.5$)

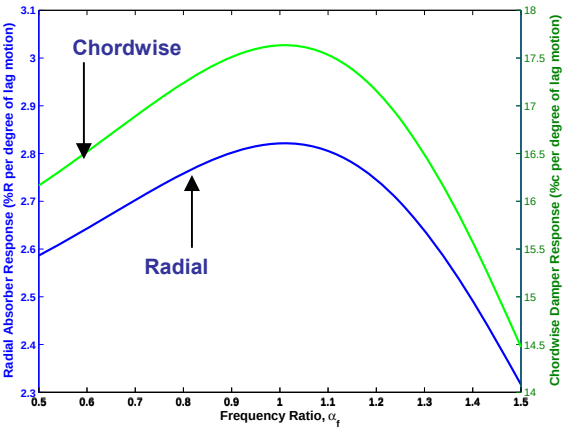

Figure 10b: 1/rev absorber amplitude per degree of lag motion ($\bar{a} = 0.7$ and $\zeta_a = 0.5$)

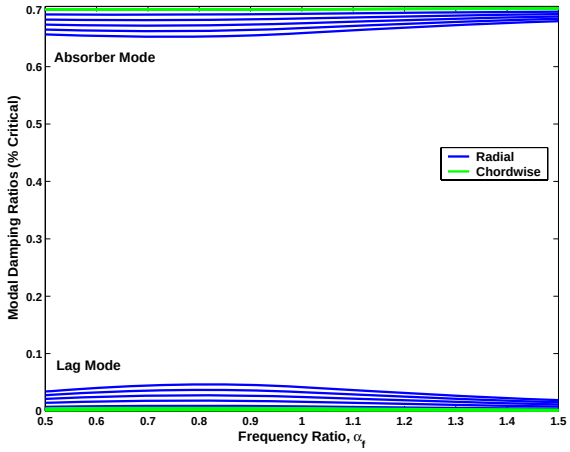

Figure 11a: Modal damping ratios vs frequency ratio, α_f ($\bar{a} = 0.3$ and $\zeta_a = 0.7$)

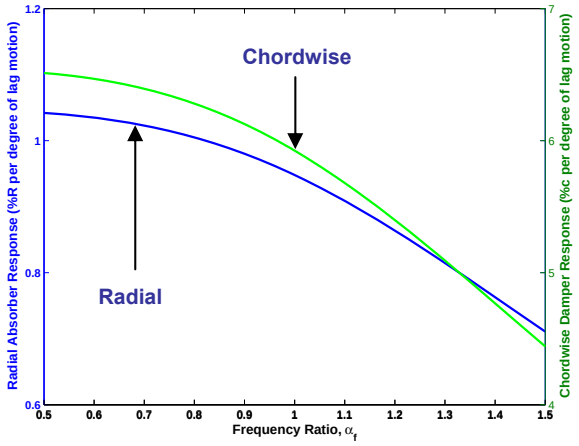

Figure 11b: 1/rev absorber amplitude per degree of lag motion ($\bar{a} = 0.3$ and $\zeta_a = 0.7$)

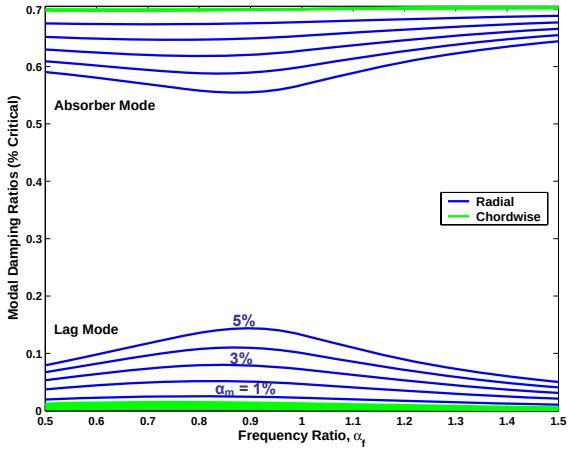

Figure 12a: Modal damping ratios vs frequency ratio, α_f ($\bar{a} = 0.5$ and $\zeta_a = 0.7$)

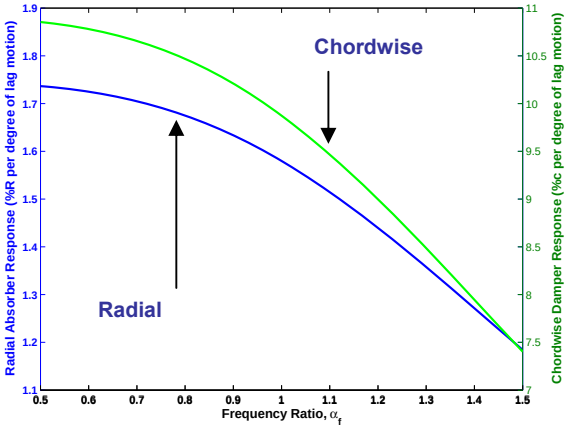

Figure 12b: 1/rev absorber amplitude per degree of lag motion ($\bar{a} = 0.5$ and $\zeta_a = 0.7$)

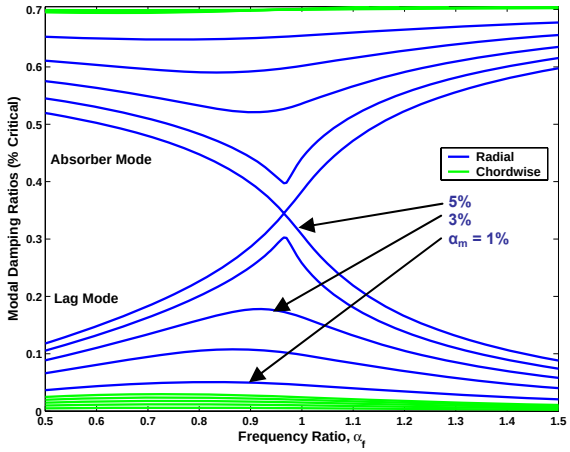

Figure 13a: Modal damping ratios vs frequency ratio, α_f ($\bar{a} = 0.7$ and $\zeta_a = 0.7$)

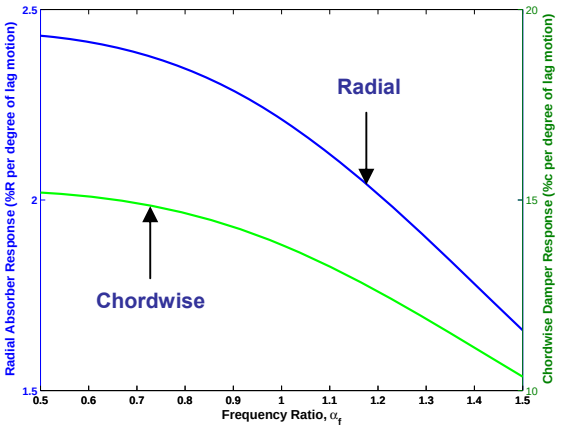

Figure 13b: 1/rev absorber amplitude per degree of lag motion ($\bar{a} = 0.7$ and $\zeta_a = 0.7$)

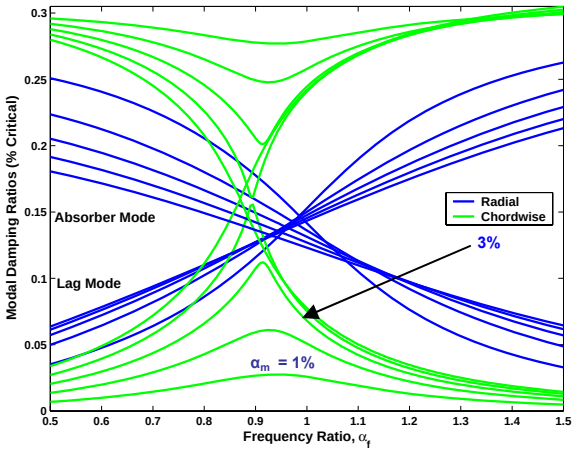

Figure 14a: Modal damping ratios vs frequency ratio, α_f ($\bar{a} = 1.0$ and $\zeta_a = 0.3$)

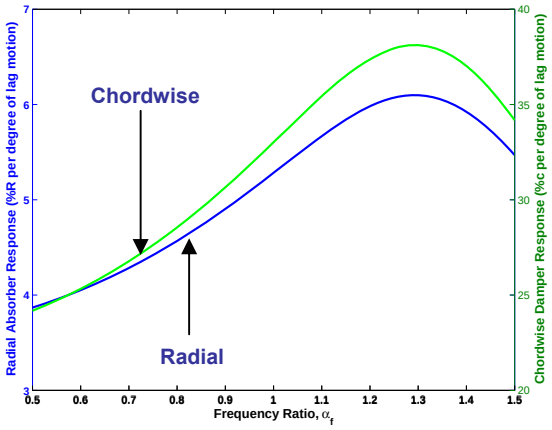

Figure 14b: 1/rev absorber amplitude per degree of lag motion ($\bar{a} = 1.0$ and $\zeta_a = 0.3$)